JOURNAL OF MATERIALS SCIENCE 31 (1996) 4811–4816

Ultrasonic study of liquid-quenched $(AgI)_x(Ag_3PO_4)_{1-x}$ compared with $(AgI)_x(Ag_4P_2O_7)_{1-x}$

A. DOI, H. HAYAKAWA, T. MIZUNO
Department of Materials, Nagoya Institute of Technology, Nagoya 466, Japan
H. KAMIOKA
Department of Physics, Faculty of Engineering, Gifu University, Gifu 501–11, Japan

The use of ultrasonic velocity–attenuation in the transition region from glassy to supercooled liquid state of the $(AgI)_x(Ag_4P_2O_7)_{1-x}$ system is extended to the $(AgI)_x(Ag_3PO_4)_{1-x}$ system. Comparison is made between both systems. The latter system is more liable to crystallize on cooling from the melt during sample preparation, possibly due to the more spherical shape of the Ag_3PO_4 molecule compared to the $Ag_4P_2O_7$ molecule (allowing easier rearrangement of the molecule for crystallization with AgI). By deliberate quenching one can escape crystallization, but only for the $x=0.75$ composition. Ultrasonics for this glass reveal structural features which are similar to those observed by differential scanning calorimetry.

1. Introduction

AgI-containing oxide glasses are known [1–4] as one of the superionic conductors having direct current (d.c.) conductivities of $\sim 10^{-2}$ S cm^{-1} at room temperature. They have been the subject of numerous fundamental as well as applied studies since the 1970s. The structure of these glasses has been suggested [5, 6] to be microscopically segregated, i.e. a mixture of microdomains of AgI and oxysalt. Their high conductivity stems from the rapid motion of Ag ions through AgI microdomains [7–9].

Recently, the authors reported ultrasonic velocity–attenuation, X-ray diffraction, differential scanning calorimetry (DSC) and density measurements on samples of the $(AgI)_x(Ag_4P_2O_7)_{1-x}$ system [10]. The ultrasonic measurements were made from room temperature to 200 °C through the glass transition temperature, T_g.

Ultrasonic studies of AgI-containing oxide glasses have been made mainly on the relaxation process of mobile silver ions at temperatures far below T_g [11–20]. Concerning the study near T_g, there are only a few reports [10, 21], partly because of the difficulty in maintaining sample shape and size in the transition region. The authors' previous study demonstrated a single attenuation peak and corresponding velocity dispersion due to relaxation of the moving units in the supercooled liquid. The purpose of the present work was to extend the study to a similar system, $(AgI)_x(Ag_3PO_4)_{1-x}$, and to compare the systems.

2. Experimental procedure

The glass-forming region in the system was reported [3] to be within $0.75 \leqslant x \leqslant 0.80$. So, four compositions of $x = 0.70$, 0.75, 0.80 and 0.85 were chosen. The experimental procedure was the same as before [10]. A mixture of AgI and Ag_3PO_4 was melted in a pyrex glass tube (which was shrouded against light with an aluminium foil) at 550 °C for 8 to 24 h in air. The melt was moulded into an aluminium tube 1 cm in height, and then polished on both ends. For ultrasonic measurements the sample thus formed was sealed with a PZT transducer of 1 MHz longitudinal wave and an aluminium buffer, was attached to another PZT transducer, and was heated in a silicone oil bath from room temperature to 200 °C at a rate of 22° h^{-1}. The transducer was activated with a pulser (Metrotec MP215) and the transmitted waves were detected with a receiver (MP106) and displayed on a digital storage oscilloscope (Philips PM3350A). The differences in pulse height and in arrival time through the dual cells, with or without a sample, enabled one to determine the attenuation, α, and the sound velocity, v, of a sample.

To supplement the ultrasonic measurements, DSC measurements were made at the same rate, 22° h^{-1}, as well as at 3° min^{-1} for comparison. In addition, X-ray (CuK_α) diffraction (XRD) measurements were made at room temperature.

As will be clarified soon, the above-mentioned melt–mould procedure for sample preparation gave rise to crystallization for all values of x. So, the

0022–2461

authors tried to enhance the quenching rate. Firstly, a melt-stuffed silica tube was quenched into liquid nitrogen, into a dry ice–methanol mixture, or into an ice–water mixture; but it fractured. Rupture of the tube could be avoided by using aluminium in place of silica. However, another difficulty appeared. When quenched into liquid nitrogen, both $x = 0.70$ and 0.75 samples were in the vitreous state but, since they contained too many cracks inside, their ultrasonic signals were too faint. When quenched into dry ice–methanol mixture, only the $x = 0.75$ samples were vitreous, but still full of cracks. A compromise was made by quenching a melt-stuffed aluminium tube into the ice–water mixture, by which one obtained glass samples, of composition $x = 0.75$, which were available for ultrasonic study. Possible contamination of the sample by aluminium was verified to be negligible, if any, by XRD and DSC analyses.

3. Results and discussion

3.1. Melt-moulded samples

Fig. 1 shows the phase diagrams of $(AgI)_x(Ag_3PO_4)_{1-x}$ (system A) and of $(AgI)_x(Ag_4P_2O_7)_{1-x}$ (system B) [22]. The glass-forming regions were reported [3] to be $0.75 \leqslant x \leqslant 0.80$ for system A and $0.75 \leqslant x \leqslant 0.85$ for system B. However, these values were for the samples quenched onto a stainless steel plate after melting at 500 °C. The authors' melt could not be quenched so rapidly, out of necessity of moulding into an aluminium tube. All the samples of system A thus prepared showed crystalline phases. On the contrary, in spite of an identical technique of sample preparation, system B produced clear glasses in a wider compositional region than reported, i.e. $0.50 \leqslant x \leqslant 0.80$ [10].

Fig. 2 shows the X-ray diffraction data for four compositions. By a finger-printing procedure one observed that the $x = 0.70$ sample contained phase III (of the composition $Ag_5I_2PO_4$, $x = 2/3$) as the dominant crystalline phase, the $x = 0.75$ sample contained phase III and phase I (of the composition $Ag_7I_4PO_4$, $x = 0.8$), the $x = 0.80$ sample contained phase I only, and the $x = 0.85$ sample contained phase I and β-AgI.

Fig. 3 shows typical DSC data measured at a heating rate of 22° h^{-1}, as well as at 3° min^{-1} for comparison. No deflection which could be assigned to T_g was detected for the samples studied. The endothermic peak at 147 °C was due to the phase transition of AgI from β (hexagonal) to α (body centred cubic, b.c.c.). For the $x = 0.70$ samples, where phase III prevailed at room temperature, some samples showed the 147 °C peak, while others did not. For other compositions one always saw the 147 °C peak; the magnitude of which grew with x. Crystalline AgI grew at the expense of the remaining glass melt, rather than by thermal decomposition of phase I and/or III; because possible decomposition of phase I into AgI and phase III at 79 °C was not detected.

The broad exothermic peak, between 130 and 137 °C for $x = 0.75$, shifted to lower temperatures with increasing AgI content, or to higher temperatures with increasing heating rate. Such behaviour is typical of nucleation and/or crystallization out of the remaining glassy phase. This peak seems to be connected with the endothermic peak at 153 °C.

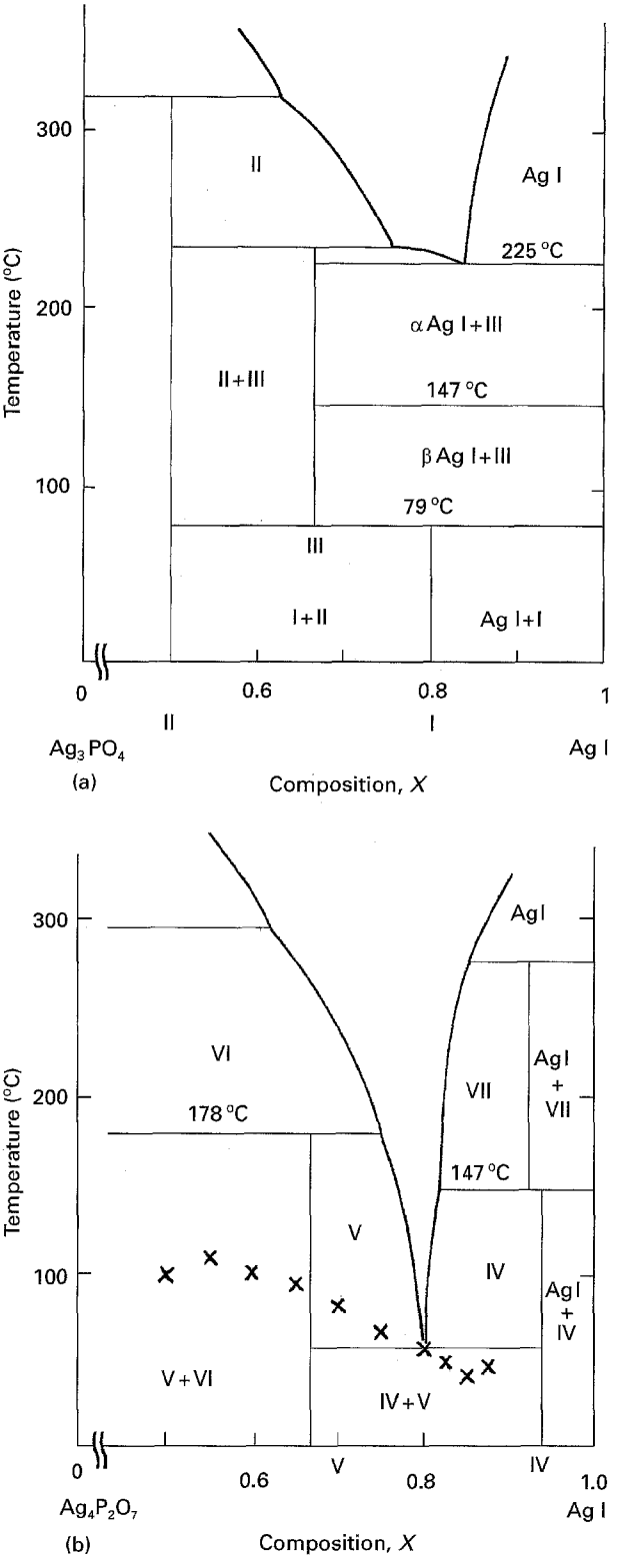

Figure 1 Phase diagrams [22] of (a) $(AgI)_x(Ag_3PO_4)_{1-x}$ and (b) $(AgI)_x(Ag_4P_2O_7)_{1-x}$ near the glass-forming regions. (×) indicate glass transition temperatures observed [10]. Phases I–VII are of the compositions $Ag_7I_4PO_4$ ($x = 0.80$), Ag_4IPO_4 ($x = 0.50$), $Ag_5I_2PO_4$ ($x = 2/3$), $Ag_{19}I_{15}P_2O_7$ ($x = 15/16$), $Ag_6I_2P_2O_7$ ($x = 2/3$), $Ag_9IP_4O_{14}$ ($x = 1/3$) and $Ag_{16}I_{12}P_2O_7$ ($x = 12/13$), respectively.

Fig. 4 shows typical ultrasonic data for four melt-moulded (and therefore devitrified) samples. In system B one observed a single attenuation peak and corresponding depression of the sound velocity, due to

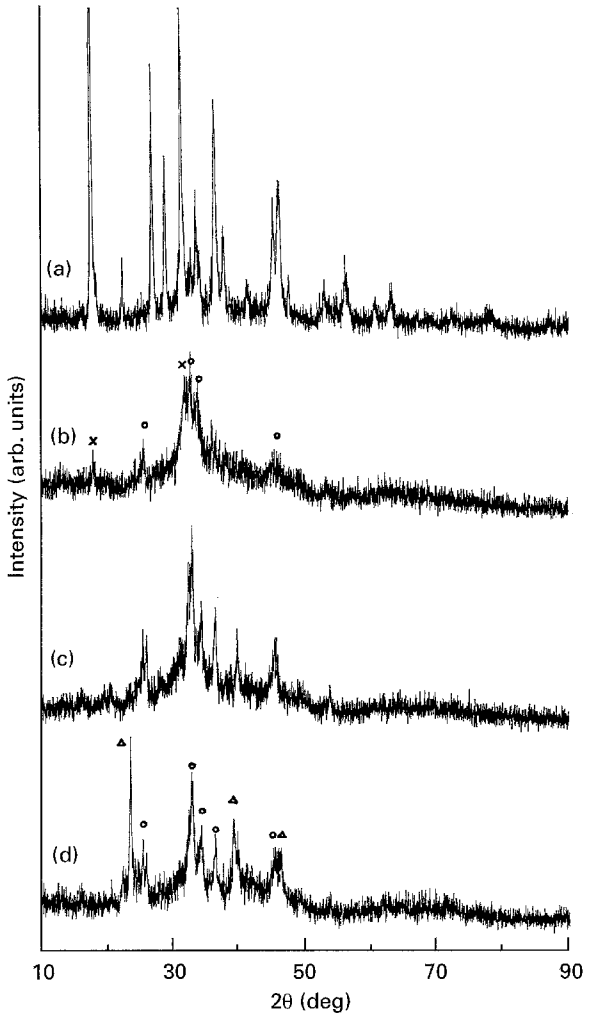

Figure 2 X-ray (CuK_α) powder diffraction of melt–moulded samples. (a) $x = 0.70$ sample showed phase III only, (b) $x = 0.75$ sample showed both phase III (×) and phase I (○) , (c) $x = 0.80$ sample showed phase I only, and (d) $x = 0.85$ sample showed both phase I(○) and β-AgI(Δ).

relaxation of the units moving in the supercooled liquid. In the authors' samples, however, the features were complex and the reproducibilities were not good. The ultrasonic technique is sensitive to structural changes, such as nucleation and/or crystallization; and is perhaps more sensitive than conventional thermal analyses [10, 23]. Therefore, observed complexities may be a reflection of some complex and subtle changes of the structure in the course of heating, especially when the sample is a composite of glassy, crystalline and molten phases.

Although the data were complex, two points of good reproducibility were noticed. First, the temperature range in which large depression of α and a corresponding large rise in v was observed, shifted to lower temperatures with increasing AgI content; i.e. 170 °C for $x = 0.70$ to 100 °C for $x = 0.85$. When a devitrified glass is heated, one expects

1. the glass transition of the remaining glassy phase and its subsequent nucleation, crystallization, phase transition and melting afterwards; and
2. the growth of the crystalline phase, phase transition and its subsequent melting, and so on.

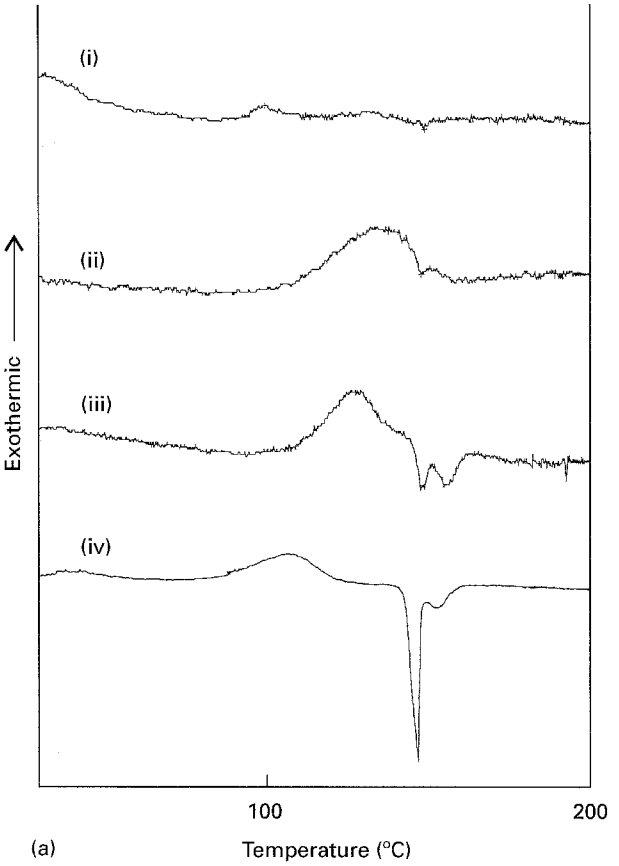

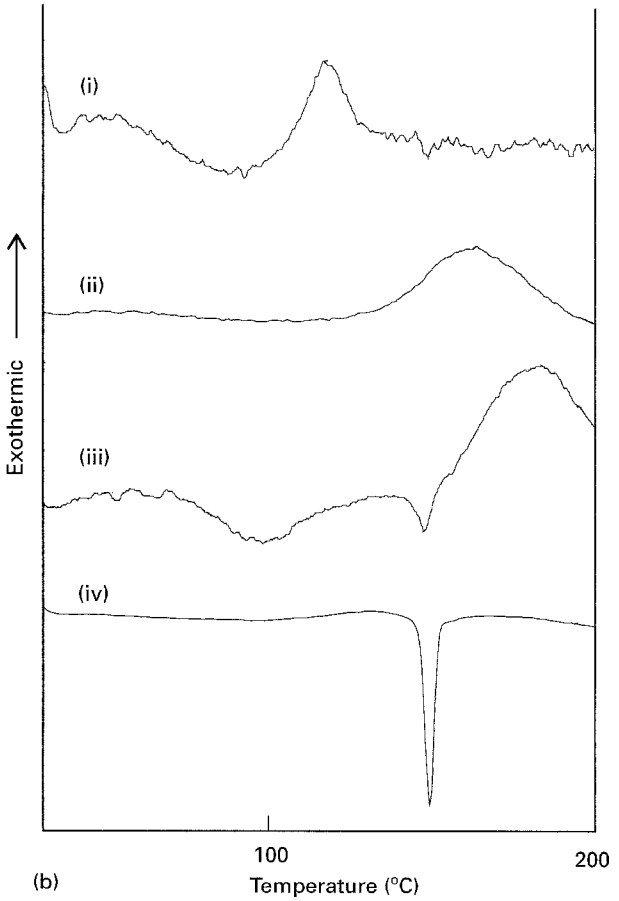

Figure 3 DSC data of four melt–moulded samples measured at heating rates of 22° h^{-1} (a), and 3° min^{-1} (b): (i) $x = 0.70$, (ii) $x = 0.75$, (iii) $x = 0.80$, (iv) $x = 0.85$. The sharp endothermic peak at 147 °C is for the β–α transition of the AgI crystal.

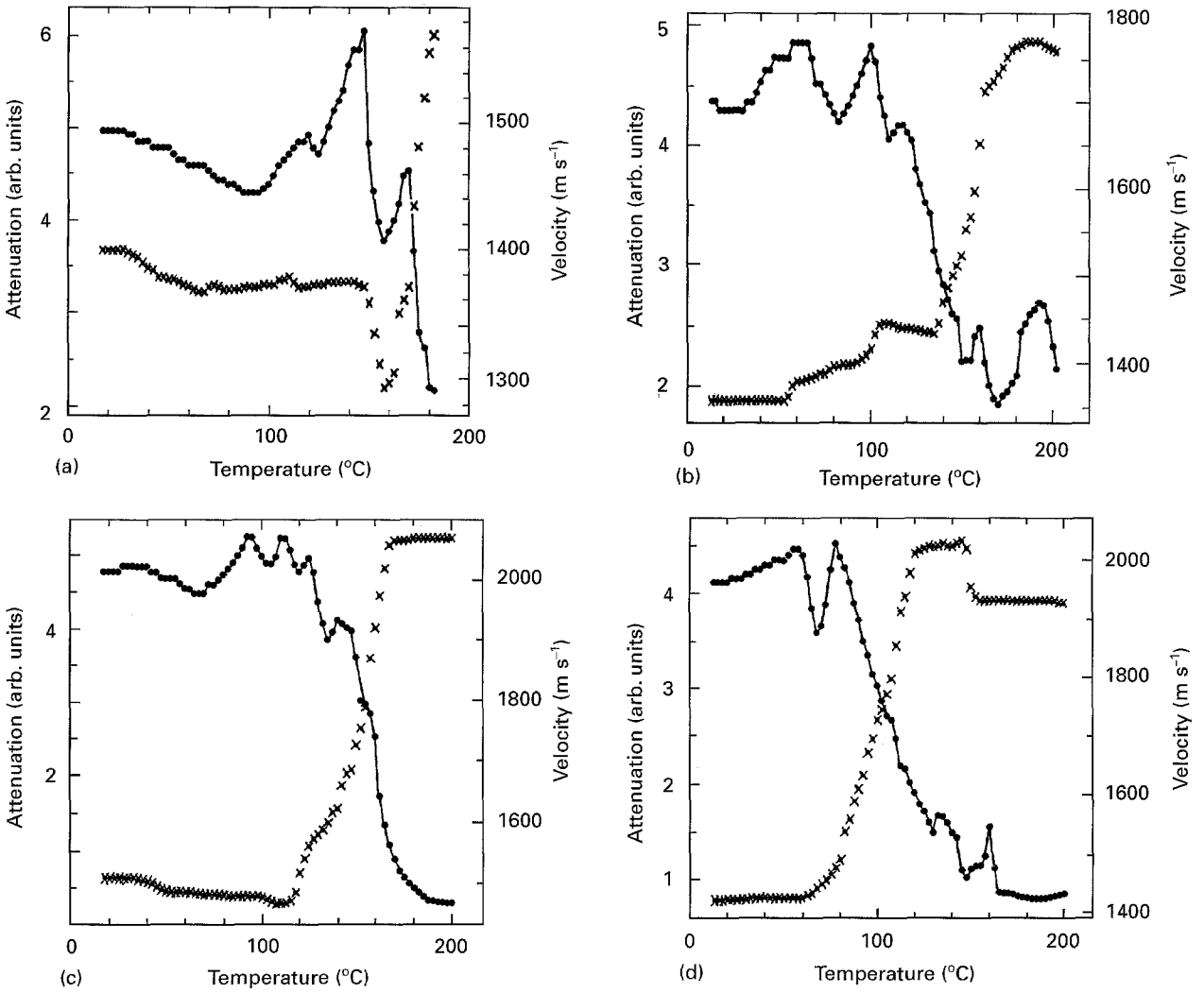

Figure 4 Typical data of ultrasonic attenuation, α(●), and velocity, v(×) for four melt–moulded (and so devitrified) samples. (a) $x = 0.70$, (b) $x = 0.75$, (c) $x = 0.80$, and (d) $x = 0.85$.

Perhaps the most plausible explanation for the observed sound anomaly may be grain growth of the crystalline phase(s). By grain growth, scattering of sound waves from the glass (or glass melt)–crystal interface would be reduced.

Second, the authors found drastic depression of v at 147 °C for the $x = 0.85$ samples. The observed behaviour can be assigned as due to β–α transition of AgI, because this crystal was abundant in samples of this composition, even at room temperature. The depression of v may be related to a 6% increase of the molar volume of the AgI crystal at this phase transition [24].

All the samples prepared by the melt–mould procedure were found to be crystalline. By enhancing the quenching rate one could obtain glass samples adequate for ultrasonic measurement, but only of the $x = 0.75$ composition. In spite of an identical melt–mould procedure for sample preparation, system B gave glasses in wider compositions. The difference between the glasses obtained from the two systems can be explained with reference to the phase diagrams (Fig. 1). In system A, the eutectic point in the measured composition range is high (225 °C) and is far higher than T_g; but in system B the eutectic is low (67 °C) and is comparable with T_g. Therefore, on cooling from the melt, system A soon enters the temperature range where stable crystal(s) can grow from the melt, unless the quenching rate is high. On the other hand, system B can be cooled down to around 67 °C without solidification. Even when it enters into the crystallization regime, the viscosity is now so high that the melt cannot but solidify to the glassy state.

In the melt of system A, the spherically shaped Ag_3PO_4 molecules rearrange easily for the formation of a compound with AgI (Fig. 5). In system B, the shape of the phosphate unit, the $Ag_4P_2O_7$ molecule, is so elongated that the necessary rearrangement of this unit for crystallization would be restricted topologically. This can be the reason why the eutectic point in system A is located high as compared to that in system B.

3.2. Quenched $x=0.75$ samples

X-ray diffraction showed that the samples were free from crystalline traces. Fig. 6 shows the DSC data measured at $\beta = 22° \, h^{-1}$. T_g was estimated to be 47 °C. The exothermic peak A, which levelled-off at around 80 °C and reached a maximum at 85 °C, was assigned to crystallization of phase III (and possibly also to β-AgI in some samples because of the presence of a faint endothermic peak, C, at around 147 °C). On

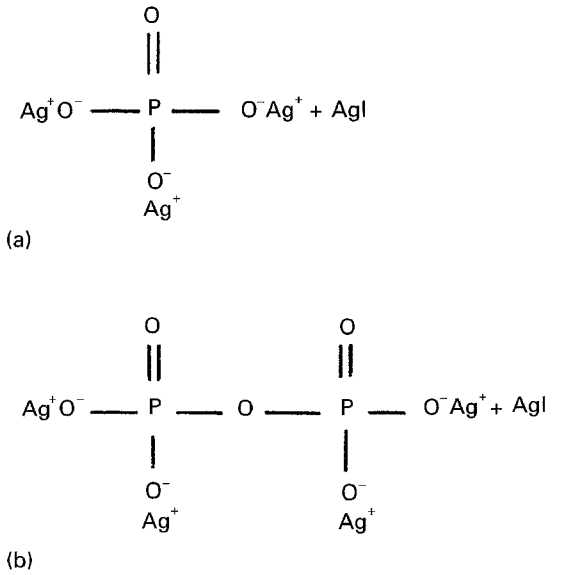

Figure 5 Structural units before melting of systems $(AgI)_x(Ag_3PO_4)_{1-x}$ (a), and $(AgI)_x(Ag_4P_2O_7)_{1-x}$ (b).

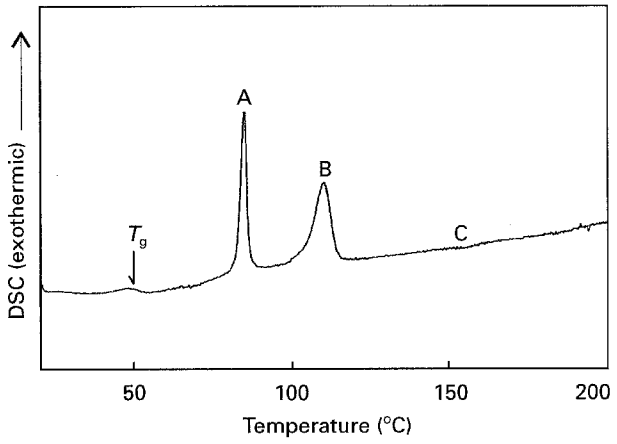

Figure 6 DSC data of the quenched $x = 0.75$ glass sample measured at a heating rate of 22° h^{-1}. The arrow indicates the glass transition temperature, T_g, while A, B and C mark positions of the DSC peaks.

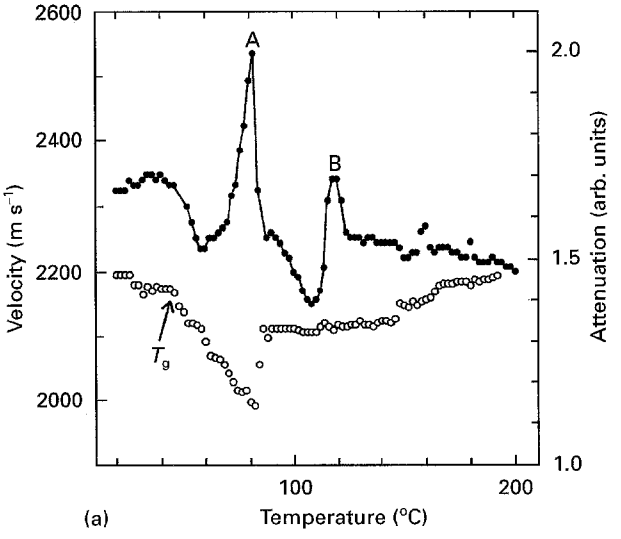

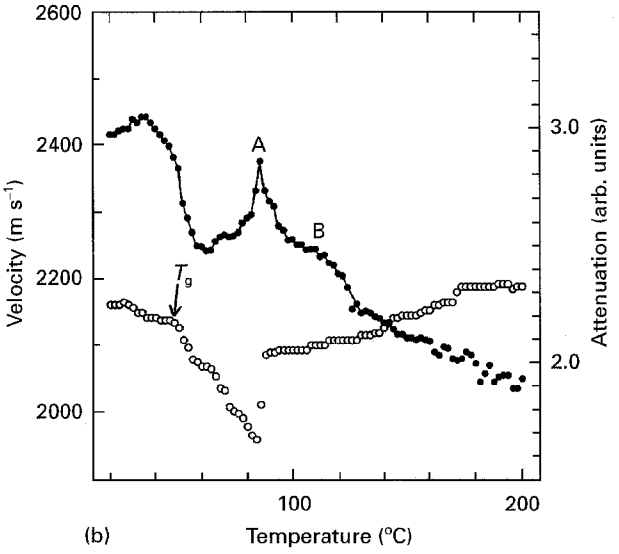

Figure 7 Ultrasonic attenuation, α(●), and velocity, v(○), for two (a and b) samples of quenched $x = 0.75$ glass. T_g marks the glass transition temperature, and A and B mark the attenuation peaks.

the other hand, the origin of the exothermic peak B with a peak maximum at 111 °C was uncertain.

Fig. 7 shows typical ultrasonic data for two quenched $x = 0.75$ samples. It is to be noted that, in such a complex system as this, one could not obtain ideal reproducibility of the shapes and sizes of the curves [10].

In the transition region from a glassy to a supercooled liquid state, one usually observed depression of the sound velocity and a corresponding attenuation peak caused by resonance of the relaxing motion of the moving units with an external stress [10]. In truth, the sound velocity depression started at T_g, but soon rose (abruptly) to a plateau at around 80 °C at which the attenuation showed peak A. This attenuation peak may correspond to the DSC peak A (Fig. 6), assigned to crystallization of phase III. This assignment may be reasonable, because the sound velocity can be enhanced by preferential transport of the sound waves through the crystalline phase. Concerning the possible attenuation peak due to glass transition, the authors believe this was obscured by the dominance of peak A, except for the tails on both sides.

The attenuation showed the second peak, B, at the same temperature as the DSC peak B; although in sample b this peak seemed to appear only as a shoulder. The authors are uncertain at present about its origin. The only clue is that the relevant phenomenon did not induce change in the sound velocity. Contrary to system B, attenuation in the glass was initially large, but depression started at T_g. This was explained by the presence of some cracks and their diminution by melting at temperatures above T_g.

4. Conclusions

Ultrasonic comparison of the samples of two systems, $(AgI)_x(Ag_3PO_4)_{1-x}$ and $(AgI)_x(Ag_4P_2O_7)_{1-x}$, melt-moulded from 550 °C to room temperature, supports the X-ray diffraction results that the former system is more liable to crystallize on cooling from the melt. By increasing the quenching rate, although with caution

not to generate cracks inside, one could obtain glassy samples for ultrasonic measurements, but only of the composition $x = 0.75$.

Ultrasonic velocity attenuation for this glass revealed a glass transition at 47 °C, the possible crystallization of phase III at around 83 °C and an unknown phenomenon at 120 °C. These ultrasonic assignments coincide well with the DSC data.

References

1. D. KUNZE, in "Fast Ion Transport in Solids", edited by W. van Gool (North-Holland, Amsterdam, 1973) p. 405.
2. G. CHIODELLI, A. MAGISTRIS and A. SCHIRALDI, *Electrochim. Acta* **19** (1974) 655.
3. T. MINAMI, Y. TAKUMA and M. TANAKA, *J. Electrochem. Soc.* **124** (1977) 1659.
4. J. P. MALUGANI, A. WASNIEWSKI, M. DOREAU and G. ROBERT, *Mater. Res. Bull.* **13** (1978) 427.
5. P. BENASSI, A. FONTANA and P. A. M. RODRIGUES, *Phys. Rev.* **B 43** (1991) 1756.
6. C. ROUSSELOT, M. TACHEZ, J. P. MALUGANI and R. MERCIER, *Solid State Ionics* **44** (1991) 151.
7. T. MINAMI, *J. Non-Cryst. Solids* **56** (1983) 15.
8. J. P. MALUGANI and R. MERCIER, *Solid State Ionics* **13** (1984) 293.
9. L. BÖRJESSON and L. M. TORELL, *Phys. Lett.* **107A** (1985) 190.
10. A. DOI, H. HAYAKAWA and H. KAMIOKA, *Phys. Rev.* **B 47** (1993) 14 136.
11. G. CARINI, M. CUTRONI, M. FEDERICO, G. GALLI and G. TRIPODO, *J. Non-Cryst. Solids* **56** (1983) 393.
12. *Idem., Phys. Rev.* **B 30** (1984) 7219.
13. G. CARINI, M. CUTRONI, M. FEDERICO and G. TRIPODO, *ibid.* **B 32** (1985) 8264.
14. R. BOGUE, R. J. SLADEK and C. LIE, *J. de Phys. Colloq.* **C10** (1985) 489.
15. G. C. M. CU, M. FE and G. TRI, *Solid State Ionics* **18/19** (1986) 415.
16. *Idem., ibid.* **18/19** (1986) 449.
17. M. CUTRONI and J. PELOUS, *ibid.* **28–30** (1988) 788.
18. R. VAITKUS, A. KEZIONIS, V. SAMULIONIS, A. ORLINKAS and V. SKRITSKIJ, *ibid.* **40/41** (1990) 922.
19. G. CARINI and G. TRIPODO, *J. Non-Cryst. Solids* **131–133** (1991) 1028.
20. R. BOGUE and R. J. SLADEK, *Phys. Rev.* **B 43** (1991) 4408.
21. L. CHEN, Y, XIAO, S. YANG, R. XUE, L. WANG and L. XIN, *Solid State Ionics* **40/41** (1990) 705.
22. T. TAKAHASHI, S. IKEDA and O. YAMAMOTO, *J. Electrochem. Soc.* **119** (1972) 477.
23. A. DOI, S. KARIYA and H. KAMIOKA, *J. Mater. Res.* **9** (1994) 3170.
24. G. BURLEY, *Acta Crystallogr.* **23** (1967) 1.

Received 22 June 1995
and accepted 18 March 1996